JOURNAL OF GEOPHYSICAL RESEARCH, VOL. 115, D07306, doi:10.1029/2009JD013005, 2010

The MOPITT version 4 CO product: Algorithm enhancements, validation, and long-term stability

M. N. Deeter,[1] D. P. Edwards,[1] J. C. Gille,[1] L. K. Emmons,[1] G. Francis,[1] S.-P. Ho,[1] D. Mao,[1] D. Masters,[1] H. Worden,[1] James R. Drummond,[2] and Paul C. Novelli[3]

Received 12 August 2009; revised 27 November 2009; accepted 9 December 2009; published 15 April 2010.

[1] Vertical profiles of carbon monoxide (CO) concentration and corresponding total column values derived from measurements made by the Measurements of Pollution in the Troposphere (MOPITT) satellite instrument are now being processed operationally with the "version 4" (V4) retrieval algorithm. This algorithm exploits the results of analyses of in situ data, chemical transport modeling, and radiative transfer modeling in the MOPITT postlaunch era. Improvements in the V4 product are evident in both clean and polluted conditions. The new products are validated using CO in situ measurements acquired from aircraft from 2000 to 2007. As determined by both retrieval simulations and observations, retrieval bias drift is typically about 1 ppbv/yr for levels in the middle troposphere and about 2 ppbv/yr in the upper troposphere. Retrieval simulations indicate that observed bias drift may be the result of gradual on-orbit changes in the instrument's modulation cell parameters.

Citation: Deeter, M. N., et al. (2010), The MOPITT version 4 CO product: Algorithm enhancements, validation, and long-term stability, *J. Geophys. Res.*, *115*, D07306, doi:10.1029/2009JD013005.

1. Introduction

[2] The Measurements of Pollution in the Troposphere (MOPITT) "version 3" (V3) product became available in 2002 and was the first satellite data set for tropospheric CO featuring long-term global coverage. Characteristics of this product [*Deeter et al.*, 2003] included (1) a retrieval algorithm based on optimal estimation principles to combine measurements with statistical background information ("a priori"); (2) a retrieval state vector that included CO volume mixing ratio (VMR) values on a fixed seven-level pressure grid; (3) a single "global" a priori profile and covariance matrix for all retrievals; (4) a measurement vector based on a subset of MOPITT's thermal-infrared (TIR) radiances; and (5) an operational radiative transfer model (MOPFAS) [*Edwards et al.*, 1999] based on prelaunch laboratory measurements of instrument parameters (such as modulation cell temperatures and pressures) and applicable mainly to atmospheric CO concentrations in a low to average range. The V3 product was extensively validated using in situ CO profiles measured from aircraft over a variety of geographical regions and in multiple field campaigns [*Emmons et al.*, 2004, 2007, 2009]. As the longest and most thoroughly validated satellite data set for CO, the V3 product was used to validate CO retrieval products for other satellite instruments including AIRS [*Warner et al.*, 2007], TES [*Luo et al.*, 2007], SCIAMACHY [*Buchwitz et al.*, 2007] and ACE-FTS [*Clerbaux et al.*, 2008].

[3] This paper describes a variety of algorithm improvements incorporated into the MOPITT version 4 product, which is now publicly available (http://wist.echo.nasa.gov). The remainder of the paper is organized as follows. Details of the V4 retrieval algorithm are described in section 2, followed by new validation results and analyses of retrieval convergence and information content in section 3. The issue of long-term bias drift in the V4 product is addressed in section 4 with analysis of both retrieval simulations and validation results. Finally, V3 and V4 results are compared in moderate and extreme pollution conditions in section 5.

2. V4 Algorithm Features

2.1. State Vector Representation

[4] The MOPITT retrieval algorithm is based on the Maximum A Posteriori (MAP) solution [*Rodgers*, 2000]. In the retrieval algorithm, the retrieval state vector x specifies which quantities are derived from some set of measurements. For both the previous V3 and new V4 algorithms, x includes the discretized CO profile, surface temperature, and surface emissivity [*Deeter et al.*, 2003]. There are significant differences, however, in the V4 representation of the CO profile. First, whereas the V3 state vector represented the CO vertical profile as a set of VMR values, the V4 state vector represents the CO profile as a set of log(VMR) values. Motivations for this change (based on in situ analyses) and its consequences with respect to the retrieval algorithm are

[1]Atmospheric Chemistry Division, National Center for Atmospheric Research, Boulder, Colorado, USA.
[2]Department of Physics and Atmospheric Science, Dalhousie University, Halifax, Nova Scotia, Canada.
[3]Earth Systems Research Laboratory, National Oceanic and Atmospheric Administration, Boulder, Colorado, USA.

0148-0227/10/2009JD013005

detailed by *Deeter et al.* [2007a]. For simplicity, the actual retrieval software relies on base-10 logarithms for log(VMR) calculations; however, the use of natural logarithms or any other logarithm base would produce identical retrieved VMR values. Second, the V4 state vector expresses the CO profile on a 10-level pressure grid instead of the seven-level grid used for V3. This change allows better representation of the vertical structure in both the CO a priori profiles and MOPITT weighting functions (i.e., the calculated sensitivities of the measurements to the state vector elements). The new V4 retrieval grid includes a floating surface level (as in V3) followed by nine uniformly spaced levels from 900 to 100 hPa. Employing a retrieval grid with uniform grid spacing (in pressure) also simplifies the physical interpretation of the retrieval averaging kernels [*Deeter et al.*, 2007b]. Averaging kernels quantify the sensitivity of the retrieved state vector to the true state vector [*Rodgers*, 2000].

2.2. A Priori

[5] The MAP solution depends explicitly on both the a priori state vector, which represents the statistically most probable state before the measurement, and the a priori covariance matrix, which describes the statistical variability relative to that state. The MAP solution $\hat{x}$ is written

$$\hat{x} = \left(C_a^{-1} + K^T C_\epsilon^{-1} K\right)^{-1} \left(C_a^{-1} x_a + K^T C_\epsilon^{-1} y\right), \tag{1}$$

where C_a is the a priori covariance matrix (described below), K is the weighting function matrix (which describes the model-calculated sensitivity of the each of the measurement vector elements to each of the elements of the state vector), and C_ϵ is the radiance error covariance matrix [*Rodgers*, 2000]. A priori information is required for all elements of the state vector, i.e., the CO profile, surface temperature, and surface emissivity.

2.2.1. CO

[6] Since a priori information makes a significant contribution to the MOPITT retrieved profiles, the validity of the a priori profile directly influences the absolute accuracy of the MOPITT product. In the MOPITT V3 product, a single a priori profile was employed for all retrievals. While this strategy ensures that features in the MOPITT product actually correspond to information in the measurements, it can yield large systematic differences between the "true" CO concentration and the retrieved value at levels where the weighting functions exhibit low sensitivity. To reduce such a priori-related errors, V4 a priori profiles are based on a monthly climatology from the global chemical transport model MOZART-4 (Model for Ozone and Related chemical Tracers, version 4). MOZART-4 simulates 100 chemical species with relatively detailed hydrocarbon chemistry [*Emmons et al.*, 2010] (also see http://gctm.acd.ucar.edu/). The monthly mean climatology was developed by averaging MOZART simulations for the period 1997–2004, with a horizontal resolution of T42 (2.8 × 2.8 deg) and 28 vertical levels, driven by meteorology from NCEP/NCAR (National Centers for Environmental Prediction/National Center for Atmospheric Research) reanalyses. Anthropogenic emissions were taken from the bottom-up POET database (available at http://www.aero.jussieu.fr/projet/ACCENT/POET.php) and were constant over the simulation. The biomass burning emissions (which are based on satellite fire counts) come from the Global Fire Emissions Database (GFED-v2) [*van der Werf et al.*, 2006]. MOZART simulation results were interpolated vertically to the 35-level MOPFAS grid. The intent of using a multiyear MOZART climatology as the MOPITT a priori was to include years of both relatively low and relatively high CO concentrations, thus reducing the sensitivity of the a priori to conditions in any particular year. While there were extreme fire events associated with the El Niño event in 1997–1998, resulting in anomalously high CO concentrations throughout the Northern Hemisphere [*Novelli et al.*, 2003], such events are cyclic and should therefore not be excluded from the average. For each retrieval, the climatology is spatially and temporally interpolated to the exact location and day of the observation. V4 a priori profiles are included in the V4 Level 2 product for each retrieval.

[7] The CO a priori covariance matrix describes the expected variability and interlevel correlations of the CO profile; this matrix quantifies the applied constraint in the optimal estimation retrieval algorithm. Diagonal elements of this matrix quantify variances at each of the pressure levels in the retrieval grid. Off-diagonal covariances describe correlations of CO variability for each pair of levels. In the V3 retrieval algorithm, where the retrieval state vector represented CO in terms of VMR, the CO a priori covariance matrix quantified VMR variability. In contrast, the V4 a priori covariance matrix describes the variability of log(VMR). Thus, because

$$\partial(ln(VMR)) = \partial(VMR)/VMR, \tag{2}$$

log(VMR) variances and covariances describe fractional (or relative) VMR variability rather than absolute VMR variability. As shown by *Deeter et al.* [2007a], analyses of in situ data sets for geographically diverse locations demonstrate that fractional VMR variability is more consistent (i.e., varies less from site to site) than absolute VMR variability. For example, regions which are typically unpolluted (on average) exhibit smaller VMR variances than CO source regions with greater mean VMR values. These observations, coupled with the realization that available observations and models are insufficient for developing a variable a priori covariance matrix applicable to all geographic regions in all seasons, led us to choose to use a single a priori covariance matrix for all V4 retrievals. For users, this choice also makes physical interpretation of the retrievals much simpler than if a variable a priori covariance matrix were employed.

[8] The V4 a priori covariance matrix C_a incorporates the same variance value C^O at all levels, with a constant correlation height P^c (expressed in pressure units) defining the off-diagonal elements [*Engelen and Stephens*, 1999]. Thus,

$$C_{a,ii} = C^0 \tag{3}$$

$$C_{a,ij} = C^0 \exp\left[-\left(p_i - p_j\right)^2 / \left(P^c\right)^2\right], \tag{4}$$

where p_i and p_j are the pressures for retrieval levels i and j, respectively. For V4, C^0 is set to $(0.30\ \log_{10}e)^2$, corresponding to a fractional VMR variability of 30%, and P^c is set to 100 hPa. The chosen value for C^0 represents weaker variability than equivalent V3 VMR-based values

[*Deeter et al.*, 2003], especially in the lower troposphere. This is reasonable since the V4 a priori covariance matrix represents variability with respect to local climatological a priori profiles rather than a single "global" a priori profile as used in the V3 retrieval algorithm. Overall, the MOZART-based V4 a priori profiles should be much closer to "truth" than the V3 global a priori profile. The relatively small value for P^c reduces the projection (or extrapolation) of information from levels where the MOPITT weighting functions are relatively strong (e.g., the midtroposphere) to levels where the weighting functions are relatively weak (e.g., the surface). The role of P^c is analyzed further in section 5.1. While approximate, these values for C^0 and P^c are generally consistent with analyses of aircraft in situ data sets at individual MOPITT validation sites.

2.2.2. Surface Parameters

[9] A priori values and variances are also required for surface temperature and surface emissivity. For surface temperature, both V3 and V4 a priori values are based on spatially and temporally interpolated surface air temperatures from the NCEP GDAS (Global Data Assimilation System) analysis. The assumed surface temperature a priori variance is 25 K^2, corresponding to an uncertainty of 5 K. Unlike V3, however, V4 a priori surface emissivity values are based on an analysis of gridded MOPITT radiances and corresponding MODIS surface temperatures [*Ho et al.*, 2005]. V3 a priori surface emissivity values were based on a published surface emissivity database coupled to a geographical database of surface type [*Deeter et al.*, 2003]. The assumed surface emissivity a priori variance for V4 is 0.0025, corresponding to an uncertainty of 0.05. This variance value is a factor of 10 smaller than the corresponding V3 value.

2.3. Radiative Transfer Modeling

[10] The MOPITT operational retrieval algorithm employs the MOPFAS radiative transfer model to simulate instrumental radiances and calculate the weighting function matrix K. MOPFAS is a regression-based radiative transfer model trained on a representative set of atmospheres derived from observations and models [*Edwards et al.*, 1999]. The ability of MOPFAS to efficiently simulate MOPITT radiances for highly diverse atmospheric states and surface parameters bears directly on the ultimate quality of MOPITT retrieval products.

2.3.1. Spectroscopic Data

[11] The spectroscopic data underlying MOPFAS has been updated for V4. MOPFAS is now based on the HITRAN 2004 database [*Rothman et al.*, 2005], together with the 2006 HITRAN water vapor update. However, changes in the forward model radiances (and MOPITT retrievals) due to these spectroscopic updates are generally small.

2.3.2. Instrument Parameters

[12] MOPFAS incorporates models of the physical states of the MOPITT Pressure Modulation Cells (PMCs) and Length Modulation Cells (LMCs) in order to calculate channel radiances. For V4, both the PMC and LMC models have been updated for consistency with the actual on-orbit cell pressure (P) and temperature (T) values observed during the mission. Specifically, values of P and T used to model the LMCs are now time-mean values based on long telemetry time series from P and T sensors onboard the instrument. For Phase 1 observations (from 2 March 2000 to 7 May 2001) acquired before the failure of one of MOPITT's two coolers, the time-mean LMC P and T are computed over the entire Phase 1 period. For Phase 2 observations (beginning August 2001 and continuing to the present), the LMC P and T time means are calculated over 2006. The year 2006 was chosen because it represents the approximate midpoint of the Phase 2 period (at the time of writing). For the PMCs, the Phase 2 P and T cycles are based on 2006 data. The shapes and relative phases of the PMC P and T cycles remain unchanged. For Phase 1, the PMC P and T values used in V4 are the same as those used in V3.

2.3.3. Regression Training Set

[13] As demonstrated in section 5.2, V3 retrievals sometimes failed systematically in strong CO source regions. Analysis revealed that such retrievals failed because retrieval iterations fell outside the bounds of the original MOPFAS regression training set. Application of MOPFAS to profiles with CO concentrations outside of the envelope defined by the training set profiles produces unreliable radiances and is therefore prohibited within MOPFAS. For V4, the MOPFAS training set was expanded in order to permit retrievals involving especially high CO VMRs. Specifically, the original training set composed of 58 profiles used in V3 [*Edwards et al.*, 1999] was expanded to 116 atmospheres. The added atmospheres were formed by scaling all of the original training set profiles by a factor of two. Retrieval simulations and case studies both indicate that this approach yields reliable retrievals of high CO profiles without degrading retrieval quality for low and moderate CO concentrations.

2.4. Radiance Subsets Used for Retrievals

[14] As mentioned in the previous section, the MOPITT instrument experienced a cooler failure approximately one and a half years after launch, which disabled Channels 1–4. Since the initial V3 Phase 1 retrieval product had been based on Channels 1, 3, and 7, the retrieval algorithm was reconfigured to only exploit Channels 5 and 7 [*Deeter et al.*, 2003]. Later studies demonstrated that the V3 Phase 2 product, based on the 5A, 5D, and 7D radiances, was comparable to the earlier Phase 1 product with respect to information content [*Deeter et al.*, 2004]. For both the Phase 1 and Phase 2 periods, V4 products are based on the same thermal infrared radiance subsets that were used for V3. Incorporation of the 6A and 6D near-infrared solar-reflectance radiances is a primary objective in the development of the next version of the operational MOPITT product [*Deeter et al.*, 2009]. For daytime observations over land, these radiances complement the thermal-infrared radiances by providing an additional constraint on the CO total column.

3. Retrieval Performance

3.1. Retrieval Convergence

[15] The fraction of clear-sky MOPITT observations leading to valid Level 2 retrieved profiles (i.e., the retrieval convergence rate) is generally higher in the V4 Level 2 product than in the V3 product. For V3, failed retrievals commonly followed one of two paths, characterized by regions of exceptionally low and high VMR. At the low extreme, the assumption of a VMR-normal probability distribution function in V3 occasionally led to negative VMR

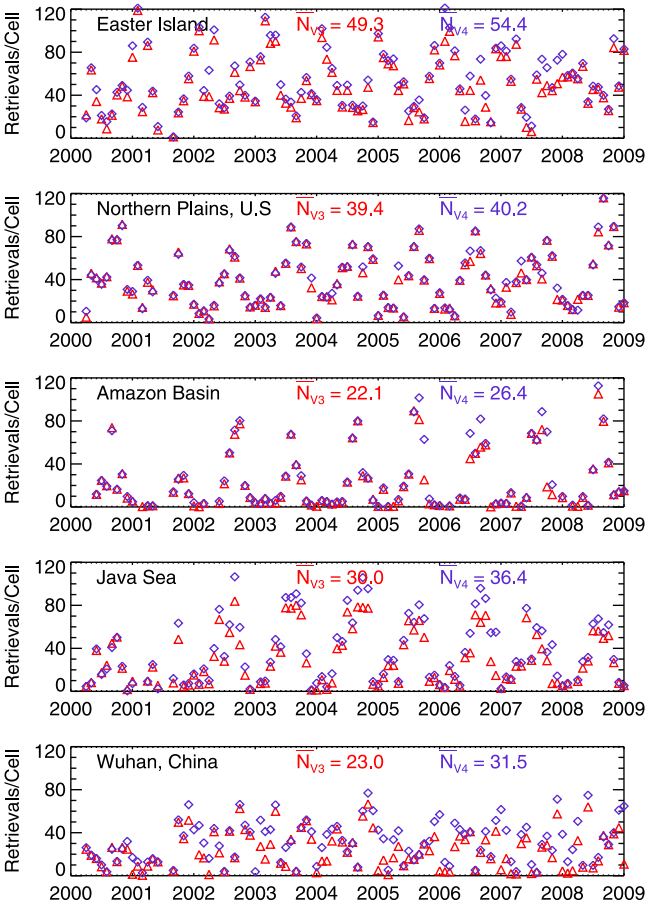

Figure 1. Time series of monthly mean number of retrievals (in units of retrievals per grid cell per month) for five contrasting sites. Easter Island represents the least polluted site, the U.S. Northern Plains reflects background conditions in the Northern Hemisphere, the Amazon Basin and Java Sea represent regions seasonally affected by biomass burning, and Wuhan is characteristic of a heavily polluted megacity.

values after inversion by the maximum a posteriori retrieval algorithm. Negative VMR values are unphysical (and incompatible with MOPFAS) and would immediately result in a failed retrieval. Conversely, in extremely polluted conditions, V3 retrievals sometimes failed because they exceeded the upper CO concentration limit of MOPFAS. In V4, these convergence problems are substantially reduced through (1) the use of log(VMR) in the retrieval state vector, which precludes negative VMR values [*Deeter et al.*, 2007a], and (2) an expanded training set for MOPFAS, which allows retrievals with significantly higher values than in V3.

[16] The improvement in retrieval convergence is demonstrated for five representative sites in the time series comparison in Figure 1. For each of the five sites, the V3 and V4 monthly mean number of retrievals were calculated over a 3 by 3 degree region corresponding to a block of nine grid cells in the gridded MOPITT Level 3 Product. The centers of the five regions are: 27.5°S, 109.5°W for Easter Island; 47.5°N, 100.5°W for the U. S. Northern Plains; 5.5° S, 65.5°W for the Amazon Basin; 4.5°S, 108.5°E for the Java Sea, and 30.5°N, 114.5°E for Wuhan, China. For each site, the overall means of both the V3 and V4 time series were also calculated and are listed near the top of each plot in Figure 1 as $\overline{N}_{V3}$ and $\overline{N}_{V4}$.

[17] The results shown in Figure 1 indicate that the improvement in retrieval convergence is highly variable, but can be readily understood. The seasonal cycle evident at most of the sites is due to clouds and is not relevant to retrieval convergence. (MOPITT retrieval products are based on clear-sky observations only.) Easter Island is located in the remote Southeastern Pacific Ocean and represents the least polluted (lowest mean CO value) of the five sites. For this site, $\overline{N}$ increases from 49.3 retrievals/cell/month for V3 to 54.4 retrievals/cell/month for V4, an increase of 10.3%. The very low CO concentrations typical of this region suggests that the increased convergence is due primarily to the log(VMR) state vector in V4, which prevents retrievals from failing due to negative VMR (as described above). For the U.S. Northern Plains site, CO concentrations generally reflect background conditions for the midlatitudes in the Northern Hemisphere, although the region is periodically affected by wildfires in Alaska, Western Canada, and the Western U.S. The small 2.0% increase in $\overline{N}$ suggests that the moderate CO concentrations typical for this site did not produce significant retrieval convergence problems in V3. The Amazon Basin and Java Sea sites are affected seasonally by strong biomass burning sources; the Java Sea region is considered further in section 5.2. For the Amazon Basin and Java Sea sites, $\overline{N}$ increases by 19.5% and 21.3%, respectively. Finally, the region of Wuhan, China represents a consistently and heavily polluted megacity. The relative increase in $\overline{N}$ observed at this site of 37.0% is the largest of the five sites. Thus, improvements in retrieval convergence in V4 are most evident in very polluted regions, but are also significant in very clean regions (e.g., in the Southern Hemisphere).

[18] However, even in the V4 product, a small fraction of retrievals may still fail. Over a full day, observed retrieval failure rates typically vary from a fraction of a percent to about two percent. The majority of these retrievals fail to converge within the maximum allowed number of iterations (which is set to 20). Retrievals failing this way tend to occur randomly, i.e., are not clustered geographically. A smaller number of retrievals fail because they yield retrieved profiles outside of the acceptable range of MOPFAS, the same problem that occurred in V3.

3.2. Validation

[19] Retrieval validation involves comparisons of actual retrieval products with values based on independent direct measurements (e.g., in situ) of the same geophysical parameter. For the purposes of validation, we consider the in situ measurements to be exact. To properly account for the "smoothing error" and influence of a priori information in the retrieval products, the true profile is transformed according to

$$x_{sim} = x_a + A(x_{true} - x_a), \tag{5}$$

where x_{sim} is the simulated retrieved profile, x_{true} is the true profile, x_a is the a priori profile, and A is the retrieval averaging kernel matrix. For V4, these quantities are defined in

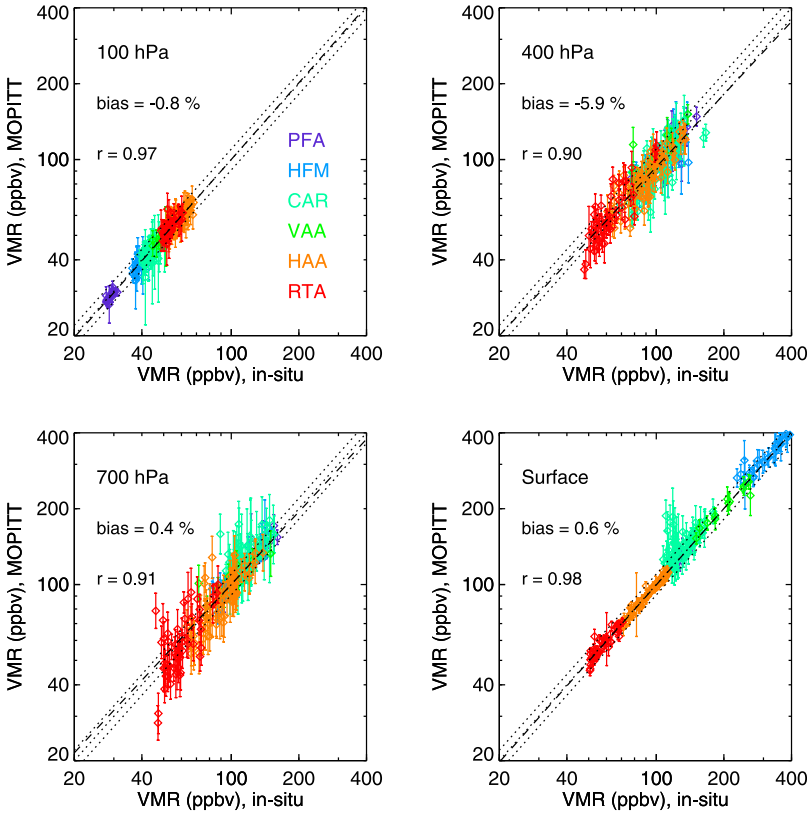

Figure 2. Scatterplots of Phase 2 retrieval validation results for surface, 700, 400, and 100 hPa levels in the MOPITT V4 product. Validation site codes are explained in section 3.2. Axes are scaled logarithmically since retrieval errors should follow lognormal distribution. Dashed lines indicate the least squares best fit. Parallel dotted lines indicate the ideal 1:1 line, as well as deviations from that line of ±10 percent.

terms of log(VMR) rather than VMR. (For validation purposes, we neglect the elements of x associated with the surface temperature and emissivity, since reliable, independent measurements of surface temperature and emissivity are not generally available.)

[20] Similar to previous MOPITT validation efforts [*emmons04*,*emmons07*,*emmons09a*], we exploit in situ profile measurements of CO acquired at six fixed sites: Rarotonga ('RTA', 21°S, 159.8°W), Hawaii ('HAA', 21.4°N, 157.2°W), Carr, Colorado ('CAR', 40.1°N, 104.1°W), Harvard Forest, Massachusetts ('HFM', 42.5°N, 71.2°W), offshore South Carolina ('VAA', 32.9°N, 79.4°W) and Poker Flat, Alaska ('PFA', 65.1°N, 147.5°W). Volume mixing ratio measurements are based on laboratory analysis of flask samples acquired in flights over the six sites. Measurements are performed and processed by the Global Monitoring Division of NOAA's Earth System Research Laboratory (ESRL). In situ data are typically acquired from near the surface up to about 300–350 hPa, limited by the aircraft's maximum altitude. In order to obtain a complete validation profile for comparison with MOPITT retrievals, each in situ profile is extrapolated vertically from the highest in situ measurement using the MOZART chemical transport model and then resampled to the MOPFAS pressure grid [*Emmons et al.*, 2004]. Scatterplots of V4 validation results are presented for Phase 2 MOPITT overpasses of these six sites in Figure 2. Retrieved log(VMR) values for observations within 100 km of the site of the acquired profiles are extracted and averaged for each overpass. Error bars indicate the associated standard deviation of the retrieved log(VMR) values for each overpass. Individual plots in Figure 2 present results for 100 hPa, 400 hPa, 700 hPa and the surface-level retrieval.

[21] For the four levels depicted, retrieved log(VMR) values exhibit excellent agreement with in situ values. Overall biases at the surface, 700, 400, and 100 hPa are 0.6%, 0.6%, −5.8%, and −0.8%, respectively. (Biases are defined as MOPITT values minus in situ values.) At both 400 and 700 hPa, where the MOPITT weighting functions and averaging kernels indicate the strongest dependence on the true CO profile, the correlation coefficient is 0.90. The large correlation coefficients at 100 hPa and at the surface (0.97 and 0.98) are mainly the result of the identical influence of the a priori profile on the actual retrieval and "simulated" retrieval (equation (5)) and are therefore not particularly significant. Confidence in the 100 hPa validation results is also tempered by the fact that above about 300 hPa both the "in situ" profile and the a priori are derived from the MOZART chemical transport model (as discussed above). V4 validation statistics for the 700 hPa level are very similar to the reported V3 results [*Emmons et al.*, 2004], whereas for 400 hPa, the V4 correlation coefficient

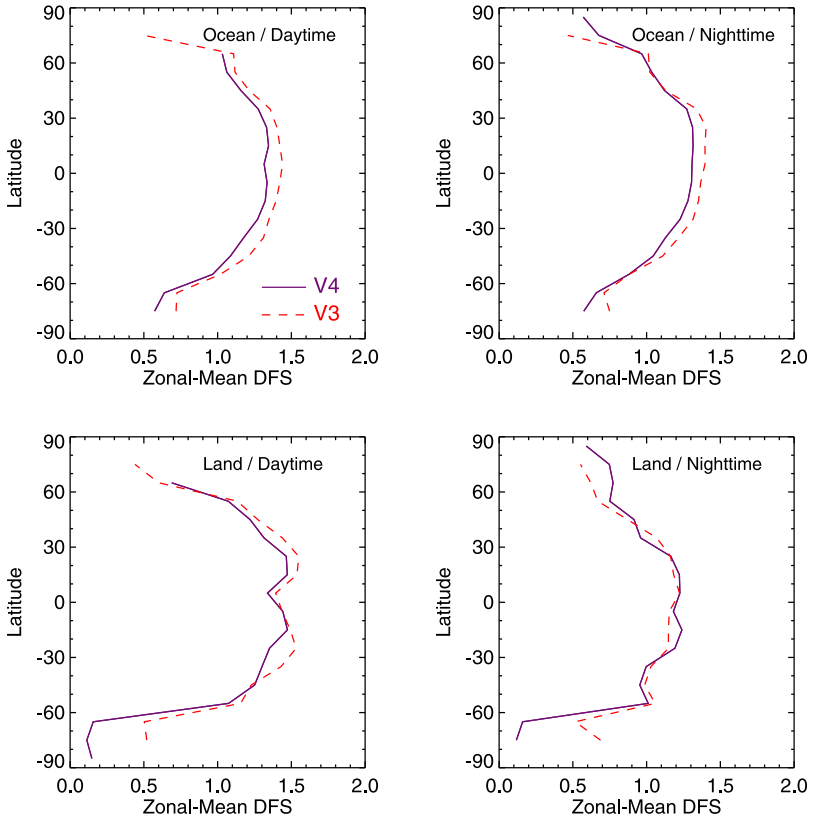

Figure 3. Comparison of zonal mean degrees of freedom for signal for MOPITT V3 products (red) and V4 products (purple) for 19 October 2006.

is somewhat larger and the bias absolute value is larger (compared to the V3 350 hPa results).

3.3. Degrees of Freedom for Signal

[22] The information content of optimal estimation-based retrieval products depends on both the strength of the constraint (i.e., the a priori covariance matrix) and on characteristics of the measurements (i.e., radiance errors and weighting functions). Representations of the V3 and V4 a priori constraints are quite different. In V3, the a priori covariance matrix was determined by calculating the VMR variability of a set of 525 in situ globally distributed profiles relative to the mean profile for the entire set [*Deeter et al.*, 2003]. Thus, the V3 a priori covariance matrix described the global variability of VMR. In V4, where the log(VMR) a priori profile varies geographically and seasonally, the a priori covariance matrix describes the relative (or fractional) variability compared to the local a priori profile. As demonstrated below, however, these fundamental differences do not lead to significant differences between the information content of V3 and V4 products.

[23] The information content of optimal estimation-based products is often quantified by the degrees of freedom for signal (DFS), which is equal to the trace of the retrieval averaging kernel matrix. DFS describes the number of pieces of independent information contained in the retrieved profile. V3 and V4 zonal mean DFS values are compared for a single day (19 October 2006) in Figure 3. The four plots separately present zonal mean DFS values for daytime observations over land, nighttime observations over land, daytime observations over ocean, and nighttime observations over ocean. Over land, daytime DFS values are typically larger than nighttime values because of thermal contrast variability [*Deeter et al.*, 2007b]. Maximum zonal mean DFS values of approximately 1.5 occur in daytime overpasses over land in the tropics. Overall, V4 DFS values are marginally smaller than V3 DFS values, and exhibit similar latitude dependence. However, the use of variable a priori profiles in V4 (instead of the global V3 a priori profile) provides a much more realistic representation of "background" CO concentrations. Thus, although slightly more information in the V4 product comes from a priori compared to V3 (as indicated by the DFS values), the a priori information is more physically realistic.

[24] While DFS is a useful index for information content, comparisons of DFS values for products from different satellite instruments measuring the same trace gas can be misleading. Since the MAP-based averaging kernel matrix depends on the a priori covariance matrix, DFS depends on retrieval algorithm parameters as well as instrumental characteristics. Specifically, as the variability defined by C_a increases, DFS increases also. Thus, unless products from different instruments are processed with the same constraint matrix, which is generally not the case, DFS comparisons cannot be used to assess the capabilities of the actual instruments. These conclusions are demonstrated by comparisons of special nonoperational MOPITT and TES CO products which were recently conducted after processing

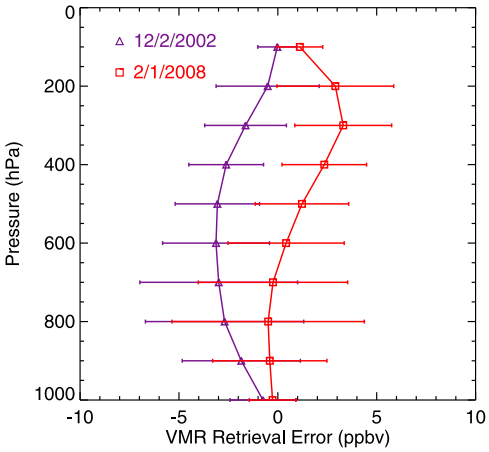

Figure 4. Simulated retrieval biases resulting from long-term changes in MOPITT instrumental parameters between 2 December 2002 and 1 February 2008.

both instruments' measurements with common a priori [*Ho et al.*, 2009].

4. Long-Term Stability

[25] As the longest satellite data set for tropospheric CO, MOPITT products will increasingly be used to quantify long-term trends. However, the use of remote sensing data sets in trend investigations makes stringent demands on long-term stability. Over the course of many years in orbit, remote sensing instruments are subject to various degrading influences. Without compensation, such instrumental changes can lead to radiance biases, i.e., errors in the forward radiative transfer model used to simulate the measurements, which can potentially propagate into retrieval biases. In the following, we consider the effect of observed long-term changes in the MOPITT correlation cell parameters which could impact retrieval bias and effectively produce long-term bias drift in the MOPITT record.

4.1. Instrumental Drift

[26] Quantitative estimates of the retrieval biases resulting from long-term drift in the operating parameters of the MOPITT length- and pressure-modulation cells were obtained through retrieval simulations based on actual instrument states for two dates separated by approximately 5 years [*Drummond et al.*, 2009]. (These results were first presented by *Emmons et al.* [2009a].) The simulations quantify the effect of exploiting a static radiative transfer model (i.e., based on fixed instrument parameters for one point in time) to process radiances produced by the instrument with perturbed instrument parameters. For these simulations, the retrieval algorithm incorporated a radiative transfer model based on MOPITT instrument parameters averaged over 2006.

[27] Two experiments were performed using a single set of reference atmospheres. Radiances were simulated over the entire set of test atmospheres for (1) an "early-mission" date (2 December 2002) and (2) a much more recent "late-mission" date (1 February 2008). These date-specific simulated radiances contain biases resulting from instrumental parameters which are known to be different than those assumed in the retrieval algorithm. The instrumental parameters used in these simulations are taken from actual MOPITT engineering data for the specified dates in 2002 and 2008 [*Drummond et al.*, 2009]. Comparisons of the simulated retrievals with the reference profiles (processed appropriately with the averaging kernels) for the two dates yields estimates of the effect of changing instrument parameters on long-term retrieval bias drift.

[28] Results of these simulations are shown in Figure 4. For the early-mission simulations, retrieval biases are typically negative and largest in the midtroposphere. At 700 hPa, the mean retrieval bias is approximately −3 ppbv. For the late-mission date, retrieval biases are typically positive and largest in the upper troposphere. At 400 hPa, the mean retrieval bias is approximately 3 ppbv. Bias drift is indicated by the difference in retrieval biases for the two dates. Inspection of Figure 4 shows that at all levels, the bias drift over the period of a little more than 5 years is positive (i.e., biases increase with time) with a maximum drift near 400 hPa of approximately 5 ppbv. In the middle troposphere (e.g., at 700 hPa), the simulated retrieval drift is approximately 3 ppbv. To summarize, this V4 simulation study indicates that long-term changes in the instrument cell parameters during Phase 2 operations should produce retrieval bias drifts of approximately 0.2 ppbv/yr in the lower stratosphere (100 hPa), 1.0 ppbv/yr in the upper troposphere (400 hPa), 0.6 ppbv/yr in the middle troposphere (700 hPa) and 0.1 ppbv/yr at the surface.

4.2. Measured Bias Drift

[29] At five of the six MOPITT validation anchor sites listed in section 3.2, in situ profile measurements have been routinely acquired (e.g., biweekly) since the beginning of the MOPITT mission. (Profile measurements for the South Carolina site began in 2004.) Retrieval biases for the 100, 400, and 700 hPa levels and the retrieved total column are plotted versus time for these validation sites in Figure 5. For each site, linear least squares fits are shown for each of the four levels. Because of possible bias discontinuities at the Phase 1–Phase 2 transition resulting from the use of different radiance subsets, fits are based on Phase 2 validation results only.

[30] At 100 hPa, the measured bias drift is only about 0.3 ppbv/yr. This value agrees well with the simulation value of 0.2 ppbv/yr. At 400 hPa, there is a clear positive bias drift of about 2 ppbv/yr at most sites which is twice as large as the simulation value. At 700 hPa, the overall bias drift is about 0.5 ppbv/yr, again in good agreement with the retrieval simulations. However, at this level, the bias drift exhibits a strong geographical dependence. For example, bias drifts at 700 hPa for individual sites vary from −2.9 ppbv/yr at Carr, Colorado to 3.5 ppbv/yr at Rarotonga. This effect is not yet well understood. Geographical variability of the retrieval bias drift might conceivably be the result of deficiencies in the NCEP water vapor product [*Trenberth et al.*, 2005] which could effectively bias the MOPITT radiances and retrievals [*Pan et al.*, 1995]. The study by Trenberth et al. demonstrates particular problems with NCEP water vapor products over the oceans, where radiosonde stations are

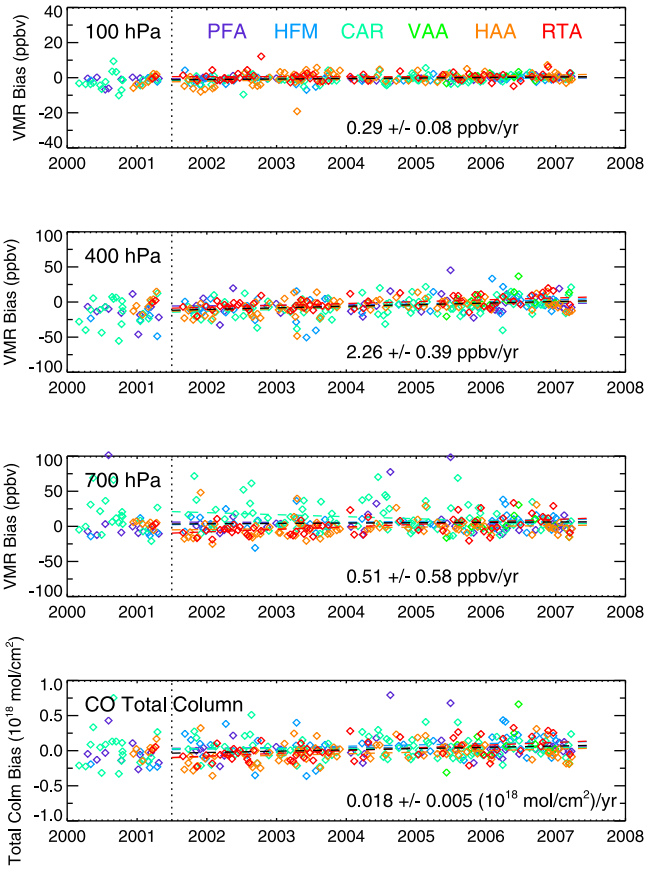

Figure 5. Time series of V4 retrieval biases determined from validation results. Least squares fits are determined using Phase 2 data only. Least squares fits were not calculated for the South Carolina (VAA) site, where regular measurements began in 2004. Overall drift (and uncertainty) values listed in each plot were determined from least squares fit to data from all sites.

sparsely distributed. With respect to the retrieved total column, the observed overall bias drift is typically about 2×10^{16} (mol/cm^2/yr).

[31] While the observed bias drift is roughly consistent with the simulation results presented in section 4.1, it should be emphasized that this does not prove definitively that long-term changes in the modulation cells are the underlying primary cause of the observed bias drift (although it seems very plausible). It is conceivable that other instrumental parameters, including some that cannot be directly monitored, might also play a significant role. In light of this uncertainty, the MOPITT Science Team chose conservatively to use a static representation of the instrument for V4 rather than attempt to explicitly account for gradual changes in the instrument's cell parameters in the forward radiative transfer model.

4.3. Surface-Station Comparisons

[32] Because MOPITT measurements (i.e., radiances) are sensitive to CO throughout the troposphere, retrieval validation is best accomplished using in situ vertical profiles. Surface-station in situ measurements are therefore generally not as useful, especially in the case of sites where MOPITT radiances are relatively insensitive to surface-level CO. However, several operational surface stations are located either at elevations or in geographic regions where MOPITT observations are sensitive to CO near the surface. Such sites include stations on isolated mountaintops and stations located in arid regions providing strong thermal contrast conditions [*Deeter et al.*, 2007b]. These sites provide additional opportunities for investigating possible long-term drifts in MOPITT products, at least with respect to the lower to mid troposphere. Here we demonstrate that long-term surface-station observations complement in situ profile measurements for characterizing long-term drift.

[33] NOAA's ESRL coordinates and archives regular surface-based measurements of several carbon cycle gases at sites distributed widely around the world (data are available at ftp.cmdl.noaa.gov/ccg/). For this study, we exploit monthly mean CO VMR values for Tenerife, Canary Islands (28.30°N, 16.48°W, 2300 m), Assekrem, Algeria (23.18°N, 5.42°E, 2728 m), Mauna Loa, Hawaii (19.53°N, 155.58°W, 3397 m), Ascension Island (7.92°S, 14.42°W, 54 m), and Cape Grim, Australia (40.68°S, 144.68°E, 94 m above sea level). With the exceptions of Cape Grim and Ascension Island, these sites are located at elevations several km higher than the surrounding terrain. These sites therefore sample CO in the free troposphere to which MOPITT radiances are also typically sensitive. Cape Grim and Ascension Island are included for comparison to represent sites where MOPITT radiances are expected to be relatively insensitive to the layer sampled by the surface stations [*Deeter et al.*, 2007b]. For these two oceanic stations, where thermal contrast between the surface and lower troposphere is typically weak, observed correlations between the MOPITT 700 hPa retrieval product and surface-station measurements depend mainly on the statistical correlation between CO concentrations at the surface and in the midtroposphere.

[34] Monthly mean MOPITT retrieved CO VMR values at 700 hPa were calculated using all daytime MOPITT retrievals within 100 km of each surface station. These values are compared with corresponding ESRL surface-station monthly mean VMR values in the time series presented in Figure 6. Linear correlation coefficients (listed in each plot in Figure 6) are relatively large (greater than or equal to 0.83) for all sites except Ascension Island. Since both the Cape Grim and the Ascension Island surface stations should be relatively insensitive to the CO layer sampled by MOPITT (as described in the previous paragraph), the data indicate that on monthly time scales, correlations between surface-level CO and midtropospheric CO are much stronger at Cape Grim than at Ascension Island. The poor correlation for Ascension Island is likely the result of CO variability driven by springtime biomass burning events in Africa [*Edwards et al.*, 2003]. Evidently, plumes in the free troposphere from such events do not typically penetrate into the marine boundary layer in this region.

[35] Differences between the MOPITT and ESRL monthly mean values, which relate to systematic bias drift, are shown in the time series in Figure 7. Difference trends vary from 0.1 ppbv/yr at Ascension Island to 2.1 ppbv/yr at Mauna Loa. The mean difference trend over all five sites is 0.9 ppbv/yr, whereas the mean trend for the three mountaintop sites is 1.1 ppbv/yr. These results further indicate that bias

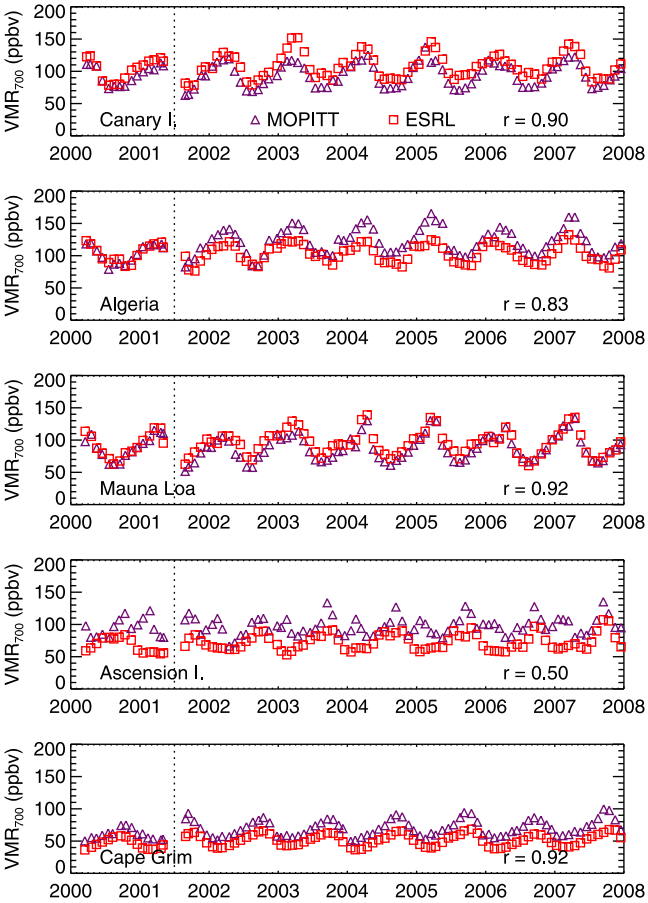

Figure 6. Comparison of MOPITT CO 700 hPa monthly means and NOAA/ESRL surface-station monthly means at five sites.

drift in the lower troposphere tends to be around 1 ppbv/yr, but also exhibits significant geographical variability.

5. Selected Results

5.1. V4 Improvements in Moderate Pollution Conditions

[36] Differences between the V3 and V4 products are highlighted in Figure 8 which presents results for a daytime MOPITT overpass of the Indian Ocean on 19 October 2006. Retrievals are drawn from the area between 5°S, 2°S, 84°E, and 87°E. At the time of the overpass this region was affected by pollution advected toward the west from intense biomass burning in Indonesia [*Logan et al.*, 2008]. Thus, this scene represents a moderately polluted tropical oceanic scene. Figure 8a compares V3 and V4 mean retrieved profiles and retrieval variability (i.e., standard deviations); V3 and V4 a priori profiles are indicated by dashed lines. The mean V4 averaging kernels (AKs) for 100, 400, and 700 hPa and the surface are shown in Figure 8b. To facilitate interpretation, the mean V4 MOPITT weighting functions for the scene are also presented in Figure 8c. (V4 weighting functions describe the sensitivity of the radiances to perturbations of log(VMR) at each level.)

[37] For the selected scene, the mean V3 and V4 retrieved profiles shown in Figure 8a are similar in the upper troposphere, but differ dramatically in the lower troposphere. Whereas V3 concentrations increase monotonically toward the surface, V4 concentrations peak around 600 hPa. At the surface, V3 retrieved VMR values are more than three times as large as V4 values. V4 VMR values depart from the a priori values most strongly between 400 and 700 hPa and are only marginally larger than the a priori values at the surface and at 100 hPa. Figure 8c demonstrates that for this particular oceanic scene the MOPITT 5A and 5D weighting functions exhibit significant sensitivity to CO between approximately 400 and 700 hPa, with vanishing sensitivity at the surface and at 100 hPa. Thus, the shape of the CO feature in the V4 retrieved profiles closely matches the shape of the 5A and 5D weighting functions. With respect to the AKs in Figure 8b, the surface-level and 100 hPa AKs are much smaller in magnitude than the 400 and 700 hPa AKs. Thus, properties of the V4 AKs and weighting functions are consistent with the observed profiles.

[38] As described in section 3.3, the V3 a priori covariance matrix was determined from a set of 525 in situ profiles drawn from many field campaigns and geographical regions [*Deeter et al.*, 2003]. Within this set of profiles, VMR variations at widely separated levels are strongly correlated, as indicated by the off-diagonal elements of the V3 a priori

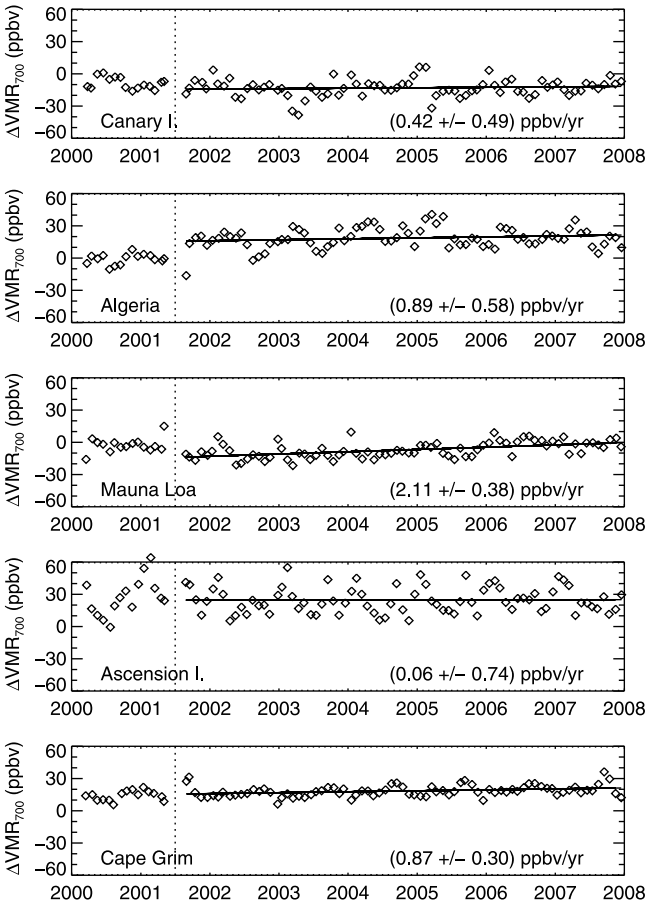

Figure 7. Time series of differences of MOPITT 700 hPa monthly means and NOAA/ESRL surface-station monthly means at five sites.

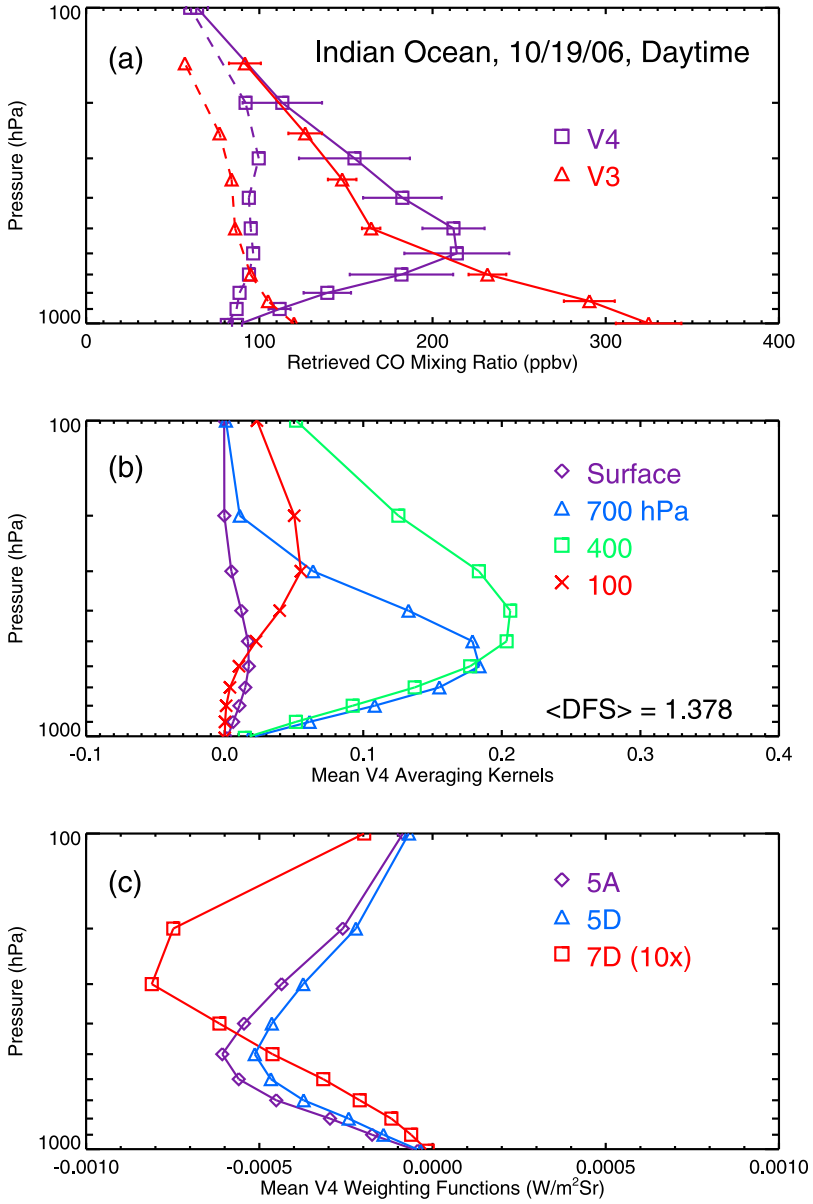

Figure 8. (a) MOPITT V3 and V4 retrieved profile statistics, (b) V4 mean averaging kernels, and (c) V4 weighting functions for daytime overpass of Indian Ocean region between 5°S, 2°S, 84°E, and 87°E on 19 October 2006. Dashed lines in Figure 8a are mean a priori profiles. The 7D weighting function in Figure 8c is scaled by a factor of 10 to aid visualization.

covariance matrix. As a result, the effective correlation length for V3 retrievals was much greater than for V4 retrievals (for which P^c = 100 hPa). The strength of interlevel correlations (as quantified by the off-diagonal elements of the a priori covariance matrix) exerts significant impact on the retrieved profiles. As the correlation length increases, differences between retrieved profiles and a priori profiles ($x - x_a$) become smoother, regardless of the characteristics of the weighting functions. As a result, retrieval levels where sensitivity is negligible can be strongly influenced by levels where the sensitivity is much stronger. In the case of oceanic scenes with low thermal contrast [*Deeter et al.*, 2007b], strong interlevel correlations can therefore "project" CO features in the midtroposphere to the surface. As the effective correlation length decreases, the surface-level retrieval should approach the a priori value.

[39] Thus, differences between V3 and V4 retrievals in Figure 8a are consistent with the different a priori covariance matrices used in the processing of the two products. Near the surface, where V3/V4 differences are largest, the V4 product more closely follows the a priori profile. Since V4 a priori values are based on a CO climatology (as discussed in section 3.3), V4 surface-level retrievals should generally be more reliable than V3 values.

5.2. V4 Improvements Near Source Regions

[40] Other improvements incorporated into the V4 product are evident near strong CO source regions. Extreme CO

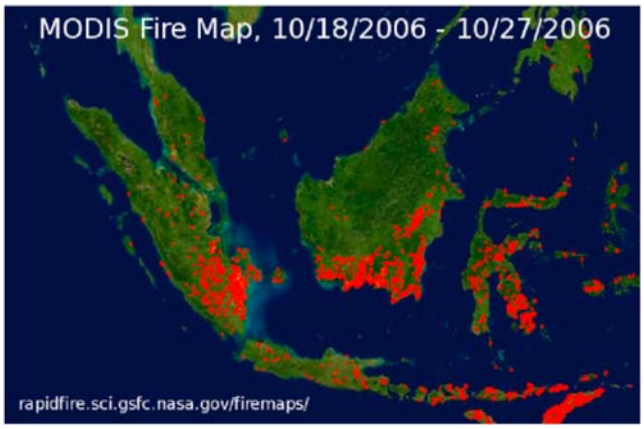

Figure 9. MODIS fire map for region bounded by 10°S, 10°N, 90°E, and 130°E based on MODIS observations between 18 and 27 October 2006.

concentrations pose a special challenge to retrieval algorithms if they are not explicitly represented in the radiative transfer modeling. The CO plume over the Indian Ocean apparent in Figure 8 on 19 October 2006 was produced by sources in Western Indonesia. Extensive fires on Borneo and Sumatra associated with an El Niño episode were the apparent source of the pollution [*Logan et al.*, 2008]. A composite fire map based on MODIS observations of the region (available at rapidfire.sci.gsfc.nasa.gov/firemaps/) from 18 to 27 October is presented in Figure 9. Composite maps of V3 and V4 retrieved CO total column products for MOPITT overpasses of the region from 19 to 21 October 2006 are compared in Figure 10. In the V3 product for these scenes, the area between Sumatra, Java, and Borneo (centered near 5°S, 110°E) reveals no valid retrievals. Analysis of the retrieval diagnostics for this region indicated that V3 retrievals in this region consistently failed because iterated VMR values exceeded the largest values in the

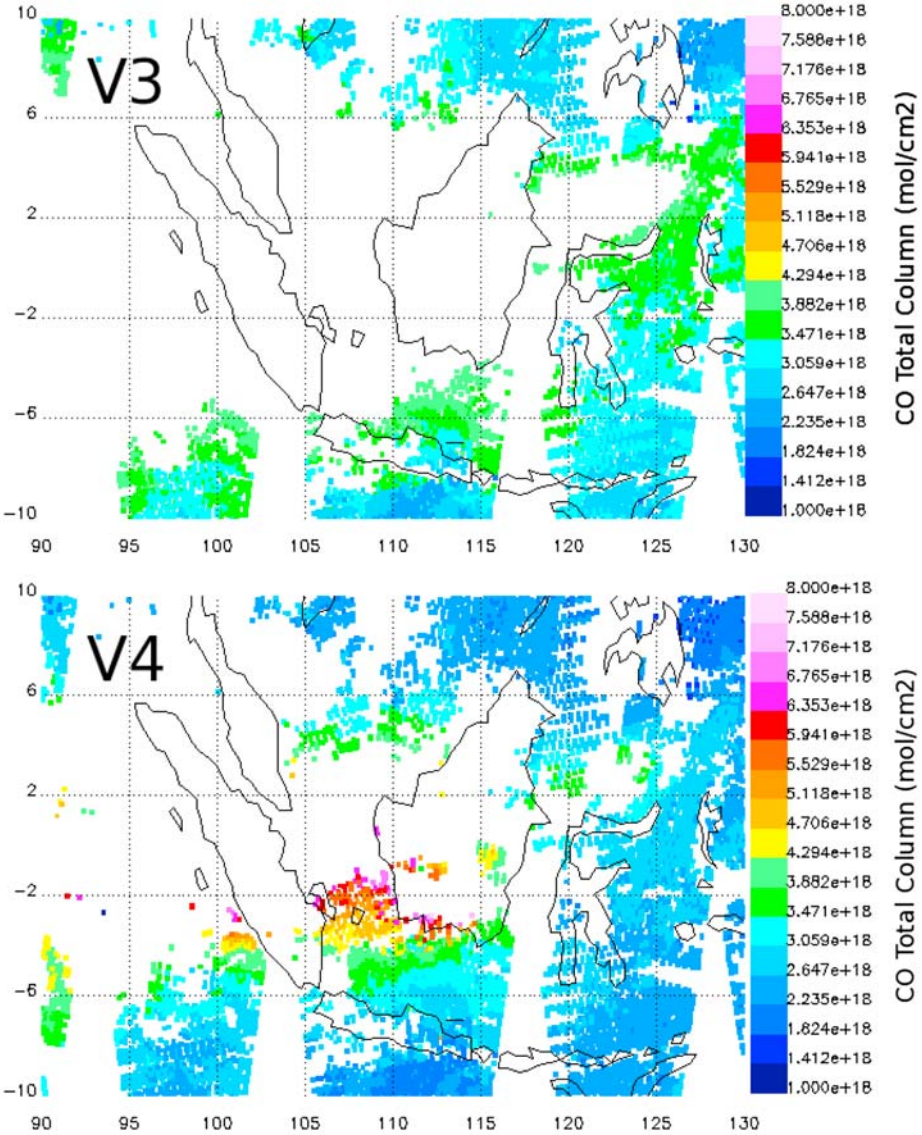

Figure 10. Comparison of V3 and V4 MOPITT total column products for overpasses of Western Indonesia between 19 and 21 October 2006.

training set used to develop MOPFAS. As the result of the expanded training set described in section 2.3, V4 results in the Figure 10 (bottom) exhibit much better retrieval convergence in this region, and expectedly reach much larger CO total column values than were possible in V3.

6. Conclusion

[41] The new MOPITT version 4 product embodies algorithm enhancements which particularly improve retrieval performance in very clean and very polluted conditions. For example, representing VMR variability in the retrieval algorithm as a lognormal quantity both reduces the possibility of retrieved VMR values being unphysically small and allows for very large VMR values in CO source regions. Similarly, extending the training set used to develop the forward radiative transfer model also facilitates retrievals in very polluted conditions. Together, these features yield daily mean retrieval convergence rates typically near 99%. With respect to retrieval product fidelity, the use of geographically and seasonally variable a priori profiles and an a priori covariance matrix with a prescribed correlation length of 100 hPa together result in more realistic retrievals at levels where MOPITT radiances are relatively insensitive to tropospheric CO.

[42] Overall, validation results based on in situ profiles acquired between 2002 and 2007 exhibit biases of less than 1% at the surface, 700 hPa, and 100 hPa, and a bias of near −6% at 400 hPa. V4 DFS values are typically slightly smaller than V3 values. Maximum zonal mean DFS values of approximately 1.5 occur in daytime overpasses over land in the Tropics. Both retrieval simulations and comparisons of MOPITT V4 data with in situ data sets indicate that retrieval bias drift is approximately 1 ppbv/yr at 700 hPa, and 2 ppbv/yr at 400 hPa. Bias drifts at 100 hPa and at the surface are negligible.

[43] Ongoing MOPITT retrieval algorithm development is focusing on three areas. First, incorporation of the MOPITT near-infrared radiances should significantly increase sensitivity to CO in the lower troposphere in daytime scenes over land. Achieving this goal is important to better characterize CO sources. The main obstacle to this objective is properly representing near-infrared radiance errors due to fine-scale spatial variability of the surface reflectance. Second, development of a forward radiative transfer model which explicitly accounts for gradual on-orbit changes in various instrumental parameters should reduce retrieval bias drift. This objective is critical to the use of future MOPITT products as climate data records. The new radiative transfer model must be thoroughly validated to ensure that the instrumental parameters which are represented as time-dependent quantities (e.g., the modulation cell temperatures and pressures) are in fact the fundamental cause of observed long-term drift in the retrieval products. As a complex instrument like MOPITT ages, the challenge of identifying and eliminating all possible sources of instrumental drift increases significantly. Finally, we are investigating whether alternative meteorological data sets, including satellite-based water vapor products, might be useful for reducing the geographical dependence of the bias drift.

[44] **Acknowledgments.** The authors acknowledge the NOAA Atmospheric Composition and Climate Change Program for supporting the surface-station in situ measurements, NASA for supporting the aircraft-based in situ measurements and the NASA/GSFC MODIS Rapid Response team for producing the fire maps. The MOPITT team would also like to acknowledge the Canadian Space Agency (CSA) for the instrument finance, the Natural Sciences and Engineering Research Council (NSERC) and Environment Canada (formerly the Meteorological Service of Canada) for help with the data processing, COMDEV (the prime contractor), and ABB BOMEM. The NCAR MOPITT project is supported by the National Aeronautics and Space Administration (NASA) Earth Observing System (EOS) Program. The National Center for Atmospheric Research (NCAR) is sponsored by the National Science Foundation.

References

Buchwitz, M., et al. (2007), Three years of global carbon monoxide from SCIAMACHY: Comparison with MOPITT and first results related to the detection of enhanced CO over cities, *Atmos. Chem. Phys.*, *7*, 2399–2411.

Clerbaux, C., et al. (2008), CO measurements from the ACE-FTS satellite instrument: Data analysis and validation using ground-based, airborne and spaceborne observations, *Atmos. Chem. Phys.*, *8*, 2569–2594.

Deeter, M. N., et al. (2003), Operational carbon monoxide retrieval algorithm and selected results for the MOPITT instrument, *J. Geophys. Res.*, *108*(D14), 4399, doi:10.1029/2002JD003186.

Deeter, M. N., L. K. Emmons, D. P. Edwards, J. C. Gille, and J. R. Drummond (2004), Vertical resolution and information content of CO profiles retrieved by MOPITT, *Geophys. Res. Lett.*, *31*, L15112, doi:10.1029/2004GL020235.

Deeter, M. N., D. P. Edwards, and J. C. Gille (2007a), Retrievals of carbon monoxide profiles from MOPITT observations using lognormal a priori statistics, *J. Geophys. Res.*, *112*, D11311, doi:10.1029/2006JD007999.

Deeter, M. N., D. P. Edwards, J. C. Gille, and J. R. Drummond (2007b), Sensitivity of MOPITT observations to carbon monoxide in the lower troposphere, *J. Geophys. Res.*, *112*, D24306, doi:10.1029/2007JD008929.

Deeter, M. N., D. P. Edwards, J. C. Gille, and J. R. Drummond (2009), CO retrievals based on MOPITT near-infrared observations, *J. Geophys. Res.*, *114*, D04303, doi:10.1029/2008JD010872.

Drummond, J. R., et al. (2009), A review of 9-year performance and operation of the MOPITT instrument, *Adv. Space Res.*, *45*, 760–774.

Edwards, D. P., C. M. Halvorson, and J. C. Gille (1999), Radiative transfer modeling for the EOS Terra satellite Measurements of Pollution in the Troposphere (MOPITT) instrument, *J. Geophys. Res.*, *104*, 16,755–16,775.

Edwards, D. P., et al. (2003), Tropospheric ozone over the tropical Atlantic: A satellite perspective, *J. Geophys. Res.*, *108*(D8), 4237, doi:10.1029/2002JD002927.

Emmons, L. K., et al. (2004), Validation of Measurements of Pollution in the Troposphere (MOPITT) CO retrievals with aircraft in situ profiles, *J. Geophys. Res.*, *109*, D03309, doi:10.1029/2003JD004101.

Emmons, L. K., et al. (2007), Measurements of Pollution in the Troposphere (MOPITT) validation exercises during summer 2004 field campaigns over North America, *J. Geophys. Res.*, *112*, D12S02, doi:10.1029/2006JD007833.

Emmons, L. K., et al. (2009), Measurements of Pollution in the Troposphere (MOPITT) validation through 2006, *Atmos. Chem. Phys.*, *9*, 1795–1803.

Emmons, L. K., et al. (2010), Description and evaluation of the Model for Ozone and Related Chemical Tracers, version 4 (MOZART-4), *Geosci. Model Dev.*, *3*, 43–67.

Engelen, R. J., and G. L. Stephens (1999), Characterization of water-vapour retrievals from TOVS/HIRS and SSM/T-2 measurements, *Q. J. R. Meteorol. Soc.*, *125*, 331–351.

Ho, S.-P., D. P. Edwards, J. C. Gille, J. Chen, D. Ziskin, G. L. Francis, M. N. Deeter, and J. R. Drummond (2005), Estimates of 4.7 um surface emissivity and their impact on the retrieval of tropospheric carbon monoxide by Measurements of Pollution in the Troposphere (MOPITT), *J. Geophys. Res.*, *110*, D21308, doi:10.1029/2005JD005946.

Ho, S.-P., D. P. Edwards, J. C. Gille, M. Luo, G. B. Osterman, S. S. Kulawik, and H. Worden (2009), A global comparison of carbon monoxide profiles and column amounts from TES and MOPITT, *J. Geophys. Res.*, *114*, D21307, doi:10.1029/2009JD012242.

Logan, J. A., I. Megretskaia, R. Nassar, L. T. Murray, L. Zhang, K. W. Bowman, H. M. Worden, and M. Luo (2008), Effects of the 2006 El Niño on tropospheric composition as revealed by data from the Tropospheric Emission Spectrometer (TES), *Geophys. Res. Lett.*, *35*, L03816, doi:10.1029/2007GL031698.

Luo, M., et al. (2007), Comparison of carbon monoxide measurements by TES and MOPITT: Influence of a priori data and instrument characteristics on nadir atmospheric species retrievals, *J. Geophys. Res.*, *112*, D09303, doi:10.1029/2006JD007663.

Novelli, P. C., K. A. Masarie, P. M. Lang, B. D. Hall, R. C. Myers, and J. W. Elkins (2003), Reanalysis of tropospheric CO trends: Effects of the 1997–1998 wildfires, *J. Geophys. Res.*, *108*(D15), 4464, doi:10.1029/2002JD003031.

Pan, L., D. P. Edwards, J. C. Gille, M. W. Smith, and J. R. Drummond (1995), Satellite remote sensing of tropospheric CO and CH_4: Forward model studies of the MOPITT instrument, *Appl. Opt.*, *34*, 6976–6988.

Rodgers, C. D. (2000), *Inverse Methods for Atmospheric Sounding, Theory and Practice*, World Sci., Singapore.

Rothman, L. S., et al. (2005), The HITRAN 2004 molecular spectroscopic database, *J. Quant. Spectrosc. Radiat. Transfer*, *96*, 139–204.

Trenberth, K., J. Fasullo, and L. Smith (2005), Trends and variability in column-integrated atmospheric water vapor. *Clim. Dyn.*, *24*, 741–758, doi:10.1007/s00382-005-0017-4.

van der Werf, G. R., et al. (2006), Interannual variability in global biomass burning emissions from 1997 to 2004, *Atmos. Chem. Phys.*, *6*, 3423–3441.

Warner, J., M. M. Comer, C. D. Barnet, W. W. McMillan, W. Wolf, E. Maddy, and G. Sachse (2007), A comparison of satellite tropospheric carbon monoxide measurements from AIRS and MOPITT during INTEX-A, *J. Geophys. Res.*, *112*, D12S17, doi:10.1029/2006JD007925.

M. N. Deeter, D. P. Edwards, L. K. Emmons, G. Francis, J. C. Gille, S.-P. Ho, D. Mao, D. Masters, and H. Worden, Atmospheric Chemistry Division, National Center for Atmospheric Research, PO Box 3000, Boulder, CO 80307, USA. (mnd@ucar.edu)

J. R. Drummond, Department of Physics and Atmospheric Science, Dalhousie University, Halifax, NS B3H 3J5, Canada.

P. C. Novelli, Earth Systems Research Laboratory, National Oceanic and Atmospheric Administration, Boulder, CO 80303, USA.